Development 134, 55-64 (2007) doi:10.1242/dev.02666

Projections of *Drosophila* multidendritic neurons in the central nervous system: links with peripheral dendrite morphology

Wesley B. Grueber[1,*,†], Bing Ye[1], Chung-Hui Yang[1], Susan Younger[2], Kelly Borden[2], Lily Y. Jan[1,2] and Yuh-Nung Jan[1,2,†]

Neurons establish diverse dendritic morphologies during development, and a major challenge is to understand how these distinct developmental programs might relate to, and influence, neuronal function. *Drosophila* dendritic arborization (da) sensory neurons display class-specific dendritic morphology with extensive coverage of the body wall. To begin to build a basis for linking dendrite structure and function in this genetic system, we analyzed da neuron axon projections in embryonic and larval stages. We found that multiple parameters of axon morphology, including dorsoventral position, midline crossing and collateral branching, correlate with dendritic morphological class. We have identified a class-specific medial-lateral layering of axons in the central nervous system formed during embryonic development, which could allow different classes of da neurons to develop differential connectivity to second-order neurons. We have examined the effect of Robo family members on class-specific axon lamination, and have also taken a forward genetic approach to identify new genes involved in axon and dendrite development. For the latter, we screened the third chromosome at high resolution in vivo for mutations that affect class IV da neuron morphology. Several known loci, as well as putative novel mutations, were identified that contribute to sensory dendrite and/or axon patterning. This collection of mutants, together with anatomical data on dendrites and axons, should begin to permit studies of dendrite diversity in a combined developmental and functional context, and also provide a foundation for understanding shared and distinct mechanisms that control axon and dendrite morphology.

KEY WORDS: *Drosophila*, Sensory map, Dendritic arborization neurons, Genetic screen, Axon targeting, Dendrite morphogenesis

INTRODUCTION

The functional distinctions between dendrites and axons impose different constraints on their morphology. Nevertheless, proper nervous system wiring would seem to require that their morphogenesis is coordinated so that the shape and position of dendritic input is appropriate for that of the axonal output, and vice versa. An example of the close link between dendritic and axonal morphology and/or function can be seen in the organization of certain sensory maps and connectivities in the brain. For example, in the *Drosophila* olfactory system, the glomerulus innervated by projection neuron (PN) dendrites is reliably predicted based on axon projection patterns in higher brain centers (Marin et al., 2002; Wong et al., 2002). POU-domain transcription factors act to specify both class-specific axon and dendrite morphology among groups of PNs, suggesting that dendrite and axon morphogenesis can be regulated together by some of the same molecules (Komiyama et al., 2003). Coordination between dendritic and axonal morphology and development within cells is likely to be a general feature of nervous system wiring. A major challenge is therefore to understand how, in the context of their distinct morphologies and cytoskeletons, dendrite and axon development can be linked with cell identity to ensure proper wiring of the nervous system.

The *Drosophila* dendritic arborization (da) sensory neurons provide a suitable system in which to study neuronal morphogenesis. These cells are positioned just below the transparent body wall in the peripheral nervous system (PNS) and branch in two dimensions (Bodmer and Jan, 1987), making it possible to study the growth and branching of whole dendritic arbors in vivo (Gao et al., 1999). The patterns of dendritic branching of da neurons have been characterized (Grueber et al., 2002; Sweeney et al., 2002) and based on branching morphology were grouped into four distinct classes (Grueber et al., 2002). The genetic programs that regulate the development and morphological diversification of these arbors are beginning to be elucidated (Brenman et al., 2001; Gao et al., 2000a; Grueber et al., 2003a; Li et al., 2004; Moore et al., 2002; Sugimura et al., 2004; Ye et al., 2004). As yet, however, there is no evidence of the functional relevance of these diverse dendritic morphologies. Establishing this connection would help to develop a system for studies of morphological development in the context of dendrite and circuit function, and perhaps allow investigations of the functional consequences of alterations in morphology produced in various mutant backgrounds.

If morphological and functional diversity are correlated, da neurons with different dendritic morphologies might project axons to different regions of the central nervous system (CNS) and thus present sensory information with spatial divergence. Elucidating the sensory axon pattern might begin to reveal the relationship between dendrite morphology and function, and also allow studies of coordinated and distinct molecular control of axonogenesis and dendritogenesis using this system. A subset of da neuron axons have

[1]Departments of Physiology and Biochemistry, [2]Howard Hughes Medical Institute, University of California, San Francisco, Rock Hall, Room GD481, 1550 4th Street, San Francisco, CA 94143, USA.

*Current address: Department of Physiology and Cellular Biophysics, Center for Neurobiology and Behavior, Columbia University, 630 W. 168th Street, P&S 11-451, New York, NY 10032, USA
[†]Authors for correspondence (e-mail: YuhNung.Jan@ucsf.edu; wg2135@columbia.edu)

Accepted 28 September 2006

been labeled in embryos and larvae and shown to project primarily to ventral regions of the neuropil, with a small subset of axons projecting more dorsally (Merritt and Whitington, 1995; Schrader and Merritt, 2000). Here we show that the axons of da neurons in different dendritic classes have distinct morphologies and organize into different layers in the CNS. To begin to examine the molecular mechanisms responsible for the specific patterns of da neuron axons and dendrites, we tested candidate genes and generated 3299 ethylmethanesulfonate (EMS)-induced lethal lines to screen axon and dendrite morphology simultaneously with high resolution. Our anatomical data, along with this collection of mutants, provide entry points for identifying novel genes and pathways that function during neuronal morphogenesis.

MATERIALS AND METHODS

Fly stocks

MARCM analysis: (1) *y w FRT19A*, (2) *hsFLP*, *tubP-Gal80*, *FRT19A*; *Gal4$^{109(2)80}$*, *UAS-mCD8::GFP*. FLP-out analysis of axonal projections: (3) *ppk-Gal4* (this study), (4) *Gal4$^{109(2)80}$* (Gao et al., 1999), (5) *hsFLP*; *Sp/CyO*; *UAS>CD2>mCD8::GFP* (Wang et al., 2004), (6) *hsFLP*; *ppk-Gal4*; *UAS>CD2>mCD8::GFP*, (7) *hsFLP;Gal4$^{109(2)80}$*; *UAS>CD2>mCD8::GFP*, (8) *Gal4$^{109(2)80}$*; *ppk-eGFP*. Axon projections in embryos: (9) *UAS-Kaede*; *ppk-eGFP*. Ectopic expression of Robo2 and Robo3: (10) *UAS-robo2* (Rajagopalan et al., 2000), (11) *UAS-robo3* (Rajagopalan et al., 2000), (12) *yw/w*; *UAS-robo2 or robo3/CyO*; *ppk-eGFP th st FRT2A/ TM6 Ubx y+*, (13) *yw*, *hsFLP*; *Gal4$^{109(2)80}$*, *UAS-mCD8::GFP*; *tubP-Gal80*, *FRT2A*.

Generation of clones

MARCM (Lee and Luo, 1999) clones were produced as previously described (Grueber et al., 2002) by mating stocks 1 and 2 or 12 and 13 above. FLP-out clones were produced by providing a 30 minute heat shock (38°C) to late embryonic and early larval progeny from matings of stocks 3 and 6 or 7 and 8 above.

Transgenic constructs

pickpocket (ppk)-Gal4 was constructed by replacing the *eGFP* portion of *ppk-eGFP* (Grueber et al., 2003b) with a *Gal4* fragment. The *Gal4* fragment was initially digested from pPTGAL (Sharma et al., 2002) as a *Hin*dIII fragment and was subsequently cloned into the *Hin*dIII site of pBlueScript (Stratagene). The final *ppk-Gal4* construct was produced by performing a three-way ligation using: (1) the *ppk* promoter released from *ppk-eGFP* as an *Eco*RI-*Kpn*I fragment; (2) *Gal4* released from pBlueScript-*Gal4* as a *Kpn*I-*Xba*I fragment; and (3) pCasper vector released from *pCasper hs-43 lacZ* digested with *Eco*RI and *Xba*I.

To generate *pUAST-Kaede*, *Kaede* cDNA (Ando et al., 2002) was excised from *pCS2+-Kaede* (courtesy of Dr A. Miyawaki) at the *Bam*HI and *Eco*RI sites and then ligated into pCDNA3.1 (Invitrogen, Carlsbad, California). It was subsequently excised from pCDNA3.1 and ligated into *pUAST* at *Kpn*I and *Xba*I sites.

Immunohistochemistry and image analysis

Immunostaining and mounting of larvae harboring MARCM clones was performed as previously described (Grueber et al., 2002; Lee and Luo, 1999). Animals with FLP-out clones were processed similarly, and immunolabeled with rabbit-anti-GFP (1:2000; kindly provided by Dr Yang Hong, UCSF), mouse anti-CD2 (1:200; Serotec, Raleigh, NC), and rat anti-mCD8 (1:100; Caltag/Invitrogen, Carlsbad, CA), and in some cases mouse anti-Fas II (Developmental Studies Hybridoma Bank, University of Iowa). Secondary antibodies used were Cy2-conjugated donkey anti-rabbit, Rhodamine Red X-conjugated donkey anti-mouse, and Cy5-conjugated donkey anti-rat all at 1:200 dilution (Jackson ImmunoResearch, West Grove, PA). Immunostained larvae were imaged on a TCS SP2 confocal microscope (Leica Microsystems, Bannockburn, IL), or a Zeiss 510 Meta (Carl Zeiss Inc., Thornwood, NY). Live imaging of mutant embryos was performed on an MRC-600 confocal microscope (Bio-Rad, Hercules, CA). Ortho views were created using LSM510 software (Carl Zeiss Inc.).

Mutagenesis

Males were fed 0.025 mol/l EMS in 1% sucrose solution according to a modified method from Lewis and Bacher (Lewis and Bacher, 1968). Mutations were mapped by standard recombination mapping using the multiply marked *ru h th st cu sr e ca* line, followed by deficiency mapping and complementation analysis with known mutant alleles.

RESULTS

Morphology of da neuron axons correlates with dendritic class

Drosophila dendritic arborization (da) neurons have been segregated into four classes (classes I-IV) that reflect arbor complexity, arbor size and the length of terminal branches (Grueber et al., 2002). The cell bodies are distributed in ventral, ventral′, lateral and dorsal clusters between the epidermis and muscles, spreading dendrites across the body wall, and axons to the ventral nerve cord (Fig. 1A). We reasoned that if morphological classes correspond to at least partially distinct sensory systems, then their axons may have divergent morphologies and target non-overlapping regions of the ventral nerve cord, where information will be relayed to second-order neurons. Previous studies have found that most da neurons arborize together in a common fascicle in the ventral CNS, with a subset, including at least some class I da neurons, projecting to more dorsal neuropil (Merritt and Whitington, 1995; Schrader and Merritt, 2000). In light of studies showing distinct morphological types of da neurons, we used mosaic analysis with a repressible cell marker (MARCM) (Lee and Luo, 1999) to examine the morphology of da neuron dendrites and axons in third instar larvae. As a MARCM driver we used *Gal4$^{109(2)80}$* (Gao et al., 1999), which labels all multidendritic (md) sensory neurons, including those belonging to the da subgroup (Fig. 1B). Owing to the sparse labeling of central neurons, the *109(2)80* driver combined with MARCM allowed us to resolve axon morphology of individual neurons (Fig. 1B).

We collected data from wild-type da neuron clones in segments A2-A7 to identify their axon projections in the CNS (n=128). Different da classes showed distinctive types of central projections. Class I neurons were unique in their projection to the dorsal neuropil (see below; n=19). Class II axons showed collateral branches (branches exiting from the main axonal trunk, although the timing of their emergence has not been determined) that were not observed in class III and IV neurons (Fig. 1C; n=27). The class I neuron vpda also showed such a branch (Fig. 1C). Class IV neurons projected axon branches across the midline, but these were only rarely observed for the other classes (Fig. 1C; n=39; we observed one case in which the v′pda class III neuron crossed the midline). Dorsal and ventral′ class IV axons crossed the midline, but axons from the ventral neuron did not. Each class IV neuron also showed a large accumulation of branches medial to the commissural/longitudinal branch bifurcation (Fig. 1C). The class III terminals extended in an anteroposterior (AP) orientation and were relatively unbranched, showing neither the collateral branches observed in class II neurons, nor contralateral projections observed among class IV neurons (Fig. 1C; n=43).

The axons of class I and class IV neurons also showed evidence of somatotopic arrangements in the CNS. The trajectory of class I neurons in the CNS mirrored the polarity of their dendrites in the periphery. Dorsal class I neurons have distinct polarity with respect to the AP body axis: dendrites of ddaD extend anteriorly and dendrites of ddaE extend posteriorly (Grueber et al., 2002). Likewise, we found that the ddaD axons extended anteriorly in the CNS, whereas the ddaE axons extended posteriorly (Fig. 1C). Among the class IV neurons, only neurons positioned in the dorsal

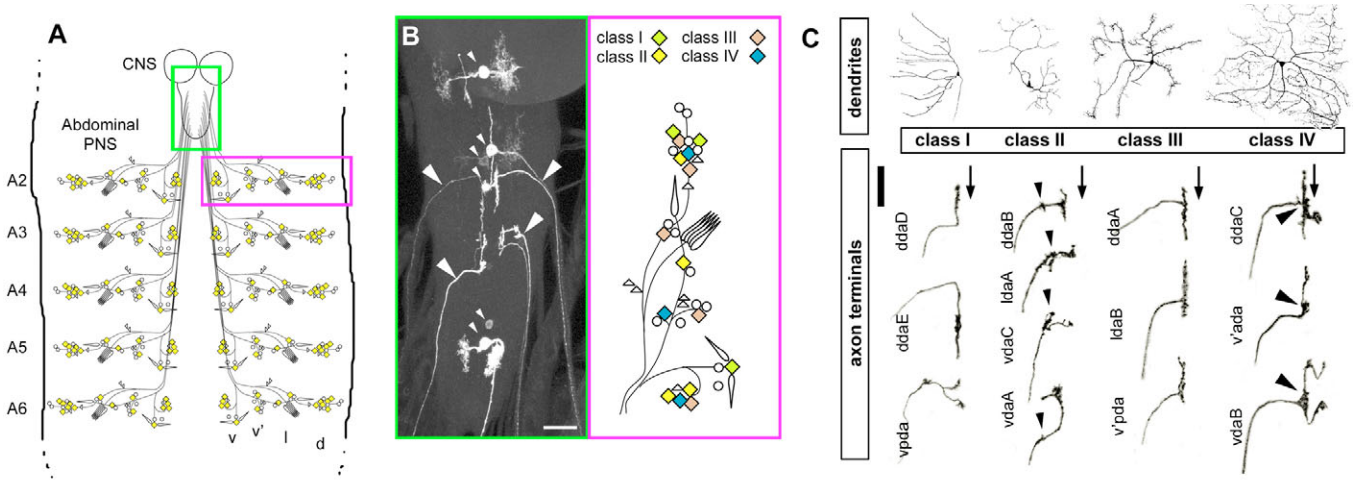

Fig. 1. Sensory axon morphology is correlated with peripheral dendritic morphology. (**A**) Schematic representation of the abdominal PNS (magenta box) and sensory axon projections to the CNS (green box). Sensory neurons are arranged in dorsal, lateral, ventral′ and ventral clusters. Segments A2-A6 are shown. (**B**) A representative dorsal view of the ventral nerve cord with sensory axons (large arrowheads) and a few central neurons (small arrowheads) labeled by the MARCM system (left, green box). Schematic of the PNS sensory neurons with dendritic arborization (da) neurons indicated by diamonds (right, magenta box). Classes of each neuron are indicated by color key: class I, green; class II, yellow; class III, tan; class IV, blue. (**C**) Top: dendritic morphologies of the four distinct classes of da neurons. Class I and II neurons have simple dendrites, with the class I dendrites directed towards the segment border. Class III neurons have numerous short dendritic protrusions extending from their main trunks. Class IV neurons have extensive and highly branched dendrites. Below: individual axon morphologies of the different classes of da neurons. Class II neurons each show collateral branches (arrowheads). Class III neurons (three of five are shown here) have simple axons without collateral branches. Dorsal and ventral class IV neurons cross the midline, and showed elaborate tufts of branches where the axon meets its anteroposterior fascicle. Arrows mark the location of axons relative to the CNS midline. Genotype: *tubP-Gal80, hsFLP, FRT19A/yw FRT19A; Gal4$^{109(2)80}$, UAS-mCD8::GFP/+*. Scale bars: 25 μm (B, axons in C). d, dorsal; l, lateral; v, ventral; v′, ventral′.

and ventral regions of the body wall, but not the lateral region, extended axons across the midline (Fig. 1C), fitting with principles of somatotopy established for body wall bristle neurons (Levine et al., 1985; Merritt and Whitington, 1995). These data together demonstrate that da neuron classes have distinguishing axon terminals, and that neurons in the same class show evidence of somatotopic organization.

Dorsoventral distinctions between axon terminals

The position of sensory axons defines the population of possible second-order targets and thus contributes strongly to sensory information processing in the CNS. Axons of tactile receptors typically project to ventral areas of the neuropil, whereas strain-sensing or proprioceptive neurons usually project to more dorsal regions (Murphey et al., 1989; Pfluger et al., 1988). Fasciclin II-labeled axon tracts provide a frame of reference for assessing dorsoventral (DV) position in the CNS (Landgraf et al., 2003) (Fig. 2A). We studied the DV positions of axons in 42 ventral nerve cords (VNCs) using MARCM, and 18 VNCs using the FLP-out system (Basler and Struhl, 1994; Wang et al., 2004; Wong et al., 2002). Both techniques revealed that each class I neuron extended axons to dorsal regions of the neuropil, terminating just lateral to the dorsomedial (DM) fascicle (Fig. 2B). The position of class I axons was therefore indistinguishable at this level of resolution from the position of the dbd terminal arbor (see Fig. 2D,E) (Zlatic et al., 2003), implying that information from class I neurons and the putative stretch-sensing dbd neuron might be processed similarly in the CNS. Class II, III and IV axons targeted the ventral CNS without obvious class-specific dorsoventral lamination of terminal position (Fig. 2C-E). The positions of the class II collateral branches were somewhat variable, either terminating on the ventrolateral (VL) fascicle (Fig. 2C), or slightly lateral to VL (vdaA often had a more lateral termination; data not shown). These data together provided anatomical support for distinct functions among different da neurons, fitting with their distinct dendritic arbor morphologies. Class II, III and IV axons project similarly to known tactile afferents, while class I neurons have projections like known proprioceptive or strain-sensing neurons.

Mediolateral lamination of axon terminals

We next examined whether the terminal positions of the ventral-projecting class II, III and IV neurons could be further distinguished by their position. Short *pickpocket* (*ppk*) enhancer sequences can drive gene expression strongly in all class IV neurons and weakly in class III neurons (Grueber et al., 2003b). Viewing all class IV neurons together revealed that they crossed the midline in a single fascicle, that the stereotyped branching at the commissural-longitudinal junction overlapped for all neurons, and that longitudinal projections were not always tightly fasciculated (Fig. 3A, Fig. 5B). In *ppk-eGFP* and *ppk-Gal4, UAS-CD8::GFP* animals, we observed a strongly labeled set of medial axons and a weakly labeled, slightly more lateral, layer of terminals (Fig. 3A). We suspected that the weakly labeled axons were class III axons, which may form a layer next to class IV axons. To test this idea, we introduced *ppk-Gal4* into the FLP-out mosaic system. We examined the relative locations of all class III axons except ddaF (whose axon was labeled too weakly) and found that their major longitudinal projections terminated immediately lateral to the scaffold of class IV axons (Fig. 3B).

The *ppk* reporter lines alone do not label the class II axons, and thus did not allow us to determine whether all da classes form a laminar organization or only the class III and IV neurons. However, examination of FLP-out clones produced with *Gal4$^{109(2)80}$*, with or without *ppk-eGFP* to label class IV neurons, permitted labeling of

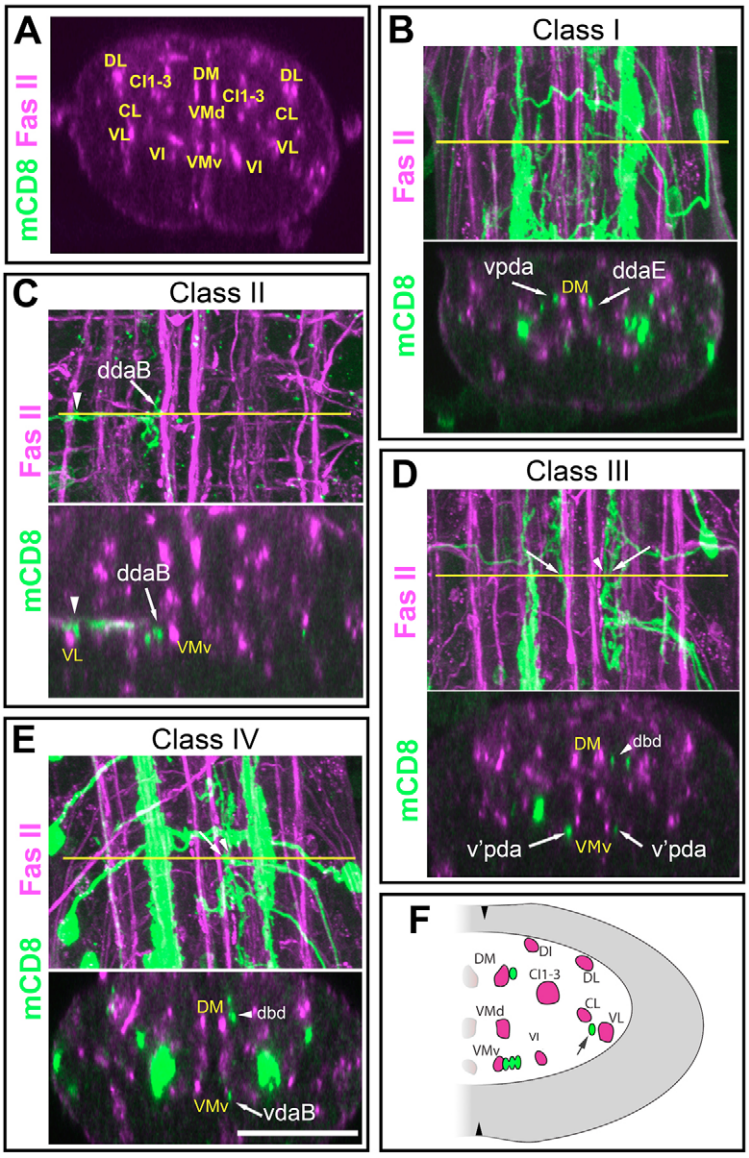

Fig. 2. Dorsoventral distinctions in axon position. (**A**) Transverse section of a wild-type ventral nerve cord labeled with Fas II antibody. Fascicle nomenclature according to Landgraf et al. (Landgraf et al., 2003). Dorsal is up in this and all other transverse sections. (**B-E**) FLP-out analysis of da neuron axon position along the DV axis. Top are dorsal views, bottom are transverse sections. Sections correspond to the location of the yellow lines. Note the position of the dbd terminal next to the DM fascicle (arrowheads in D and E). (B) The terminations of vpda and ddaE, both class I neurons, are likewise immediately next to the DM fascicle. (C) The class II neuron ddaB terminates in ventral neuropil next to VMv (arrow) and forms a collateral branch at VL (arrowhead). (D) The class III neuron v'pda terminates ventrally, adjacent to VMv (arrows). Notice that the dbd neuron next to DM (arrowheads). (E) The class IV neuron, vdaB, terminates ventrally, immediately next to VMv (arrows). (**F**) Schematic drawing of one half of a CNS section as in A, showing the positions of major fascicles and the approximate locations of da axons (green). Arrow indicates distinct lateral branch of class II neurons. Arrowheads indicate the midline. Genotypes: *hsFLP/+; Gal4*$^{109(2)80}$*/+; UAS>CD2>mCD8::GFP/+*. Scale bar: 25 μm. C, central; D, dorsal; I, intermediate; L, lateral; M, median; V, ventral.

different axon groups. We found that class II neurons with a significant longitudinal projection formed a third layer of sensory axons that was lateral to both class III (Fig. 3C) and class IV axons (Fig. 3D), with class II collateral branches terminating in a distinct, even more lateral, position (Fig. 2C).

We confirmed the FLP-out data by mapping the relationships of individual pairs of sensory afferents using the MARCM technique. Within hemisegments, or in adjacent hemisegments, having two or more da neuron clones (n=15) axons were organized (medial>lateral) class IV>class III>class II (Fig. 3E). Laminar patterning was independent of peripheral cell body position (Fig. 3E). These data together indicate the presence of a laminar arrangement of somatosensory axons in the *Drosophila* CNS. These data also suggest that somatosensory information carried by different classes of da neurons might be distinguished by sensory axon connectivity to second-order targets.

Embryonic formation of the laminar pattern

The above FLP-out and MARCM data were collected from third instar larval stages, so we next examined when during development we could observe layering of the different classes of axons. To achieve live two-color discrimination of different neuronal classes in embryonic and early larval stages we generated transgenic flies expressing a photoconvertible fluorescent protein, Kaede (Ando et al., 2002), and placed expression under the control of *Gal4*$^{109(2)80}$ in the presence of *ppk-eGFP* (Fig. 4A,A′). We converted the Kaede protein from green to red fluorescence using a 10-30 second UV pulse and examined the position of all da axons relative to *ppk-eGFP*-labeled class IV axons. As early as the sensory axon scaffold could be visualized (stage 17), class IV axons occupied a medialmost layer with respect to other classes (Fig. 4B,C). These data indicate that a laminar pattern develops at least by late embryonic stages and is maintained without qualitative change in larvae.

Alteration in md neuron axon morphology by Robo family members

Our anatomical data revealed several features of da neuron axon projections that correlated with previously described dendritic classes, including mediolateral position, midline crossing, presence or absence of collateral branches, and relative position in the DV axis. Because of the role of Robo receptors in specifying

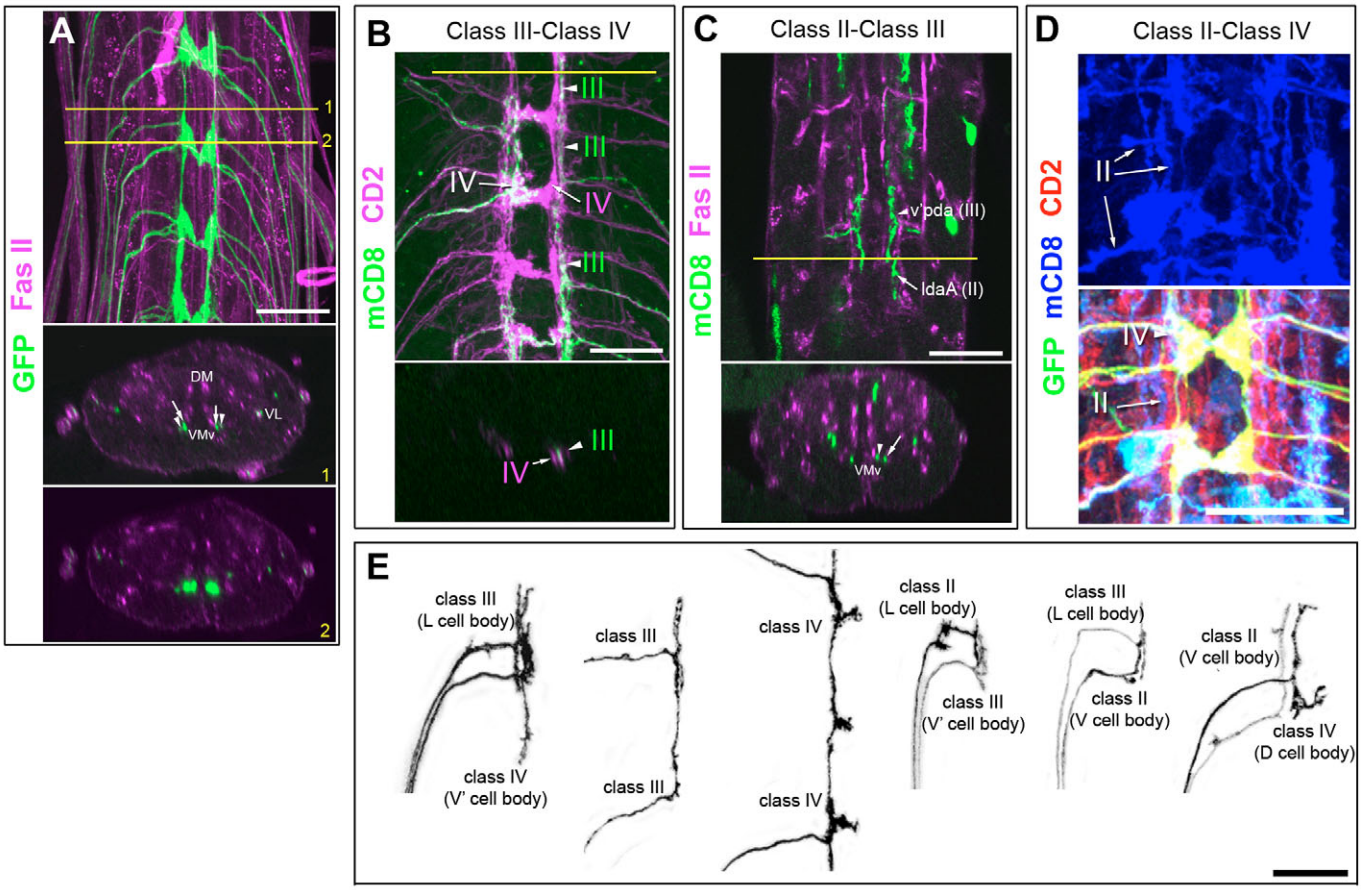

Fig. 3. Axons of different classes of da neurons form a laminar pattern. (**A**) Dorsal view of axon scaffold in *ppk-Gal4, UAS-mCD8::GFP* ventral nerve cord. A strongly labeled set of axons (arrow in transverse section '1') is flanked by a weakly labeled set of terminals (arrowheads). Transverse section '2' shows the thickened clumps of axons at each segment. (**B**) FLP-out analysis shows that class III axons (arrowheads) terminate immediately lateral to the scaffold of class IV axons (arrows). Top is dorsal view, bottom is transverse section. Notice that some class IV axons show expression of mCD8::GFP due to FLP-out and, thus, the left portion of the CNS contains marked class III and IV neurons. (**C**) Image of CNS labeled with mCD8 (green) and Fas II (magenta). Section (yellow) shows the class III axon of v'pda (arrowhead) terminating just medial to the class II axon of ldaA (arrow). (**D**) FLP-out clones made with *ppk-eGFP* in the background to label class IV axons. Arrows indicate the class II axon. The *ppk-eGFP* scaffold is marked (IV). Notice that the class II axon terminates lateral to the class IV scaffold (arrowhead) and all other da axons (which are labeled by CD2). (**E**) Relative terminal positions of class II, III and IV neurons. The cell body position is indicated along with the class of the neuron. Genotypes: (B) *hsFLP/+; ppk-Gal4/ppk-Gal4; UAS>CD2>mCD8::GFP/+*; (C) *hsFLP/+; Gal4*$^{109(2)80}$*/+; UAS>CD2>mCD8::GFP/+*. (D) *hsFLP/+; Gal4*$^{109(2)80}$*/+; UAS>CD2>mCD8::GFP/ppk-eGFP*; (E) *tubP-Gal80, hsFLP, FRT19A/yw FRT19A; Gal4*$^{109(2)80}$*, UAS-mCD8::GFP/+*. Scale bars: 25 μm. D, dorsal; L, lateral; V, ventral; V′, ventral′.

longitudinal position in the VNC (Simpson et al., 2000; Rajagopalan et al., 2000; Zlatic et al., 2003), we examined the possible functions of these genes in sensory axons. Loss of either Robo, Robo2 or Robo3 caused severe (Robo) or mild (Robos 2 and 3) alteration in sensory axon morphology (Fig. 5A). Due to the widespread regulation of VNC patterning by Robo family members (Rajagopalan et al., 2000; Simpson et al., 2000) these defects could arise by autonomous or non-autonomous regulation of sensory arbor morphology. We found that misexpression of Robo3, but not Robo2, under the control of *Gal4*$^{109(2)80}$ induced axon mistargeting and ectopic branching of class IV axons primarily along the VL fascicle (Fig. 5B), the normal position of collaterals of class II axons (Fig. 2C). MARCM-based overexpression of Robo3 indicated that this branching phenotype was cell autonomous (90%; n=20; Fig. 5C). Furthermore, class III neurons showed ectopic collateral branching (86%; n=14; Fig. 5C), and class II axons either truncated at the approximate location of their normal collateral branches, or turned from a more medial position and projected laterally to outer neuropil (60%; n=10; Fig. 5C). Neither Robo2 nor Robo3 overexpression under the control of *Gal4*$^{109(2)80}$ caused obvious shifts of the relative laminar position of da axon terminals (Fig. 5C). Robo3-overexpressing class III axons occasionally (21%; n=14) extended longitudinal branches that were separated from the class IV scaffold by a gap, which could indicate a shift to an outer layer. We next examined the distribution of Robo3 protein in the PNS. Expression was observed in chordotonal organs, as previously described (Zlatic et al., 2003), and weakly in other cells in the periphery (data not shown). We could not resolve a class-specific expression in the md neurons, but also cannot exclude low-level expression in some of these cells. Together, these results support the view that Robo family members can regulate sensory axon morphology and can modify class-specific features of md arbors (Zlatic et al., 2003). Furthermore, although a Robo code may regulate the broad location of sensory arbors, it appears not to determine the laminar pattern of the different da classes alone.

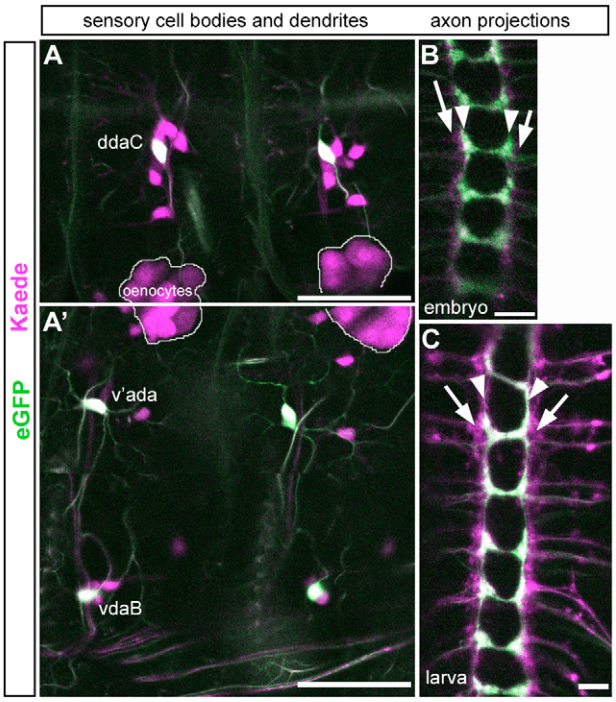

Fig. 4. Embryonic origin of laminar pattern. (**A**,**A′**) Expression of *ppk-eGFP* in larval class IV sensory cell bodies, dendrites and axons, and expression of photoconverted Kaede protein under the control of *Gal4*$^{109(2)80}$ to label all da neurons. Labeled oenocytes are encircled. (**B**) Dorsal view of stage 17 embryonic scaffold of class IV axons (arrowhead) flanked on both sides by other da axons expressing red Kaede protein (arrows). (**C**) The laminar pattern of class IV neurons (arrowhead) and other da neuron (arrow) in early larval stages. Scale bars: 50 μm in A,A′; 10 μm in B,C.

A forward genetic screen to identify regulators of axon and dendrite morphology

We next took an unbiased forward genetic approach to identify genes that regulate the morphology of axons and dendrites, using the stereotyped pattern of class IV neurons as an assay. We screened 3299 EMS-induced lines marked with *ppk-eGFP* in late embryos and early first instar larvae. The wild-type pattern of class IV axons in embryos was a simple ladder-like scaffold of longitudinal and commissural branches (Fig. 6A). From the first-round of screening, we identified 68 lines with defects in this axon pattern that did not show pronounced changes in neuron number or obvious embryonic patterning defects, such as missing or fused segments. We recovered several mutants that showed dendrite-specific phenotypes (B.Y., W.B.G., S.Y., L.Y.J., Y-N.J., unpublished), and 25 mutants showing aberrant dendrite and axon morphology. Although we have not investigated the cell autonomy or non-autonomy of these phenotypes, the mutations recovered suggest that dendritic and axonal morphogenesis proceed by both common and distinct molecular mechanisms. Here we introduce a subset of the mutations that may be relevant to understanding mechanisms of sensory axon patterning.

We identified several mutant lines with disrupted class IV longitudinal or commissural projections (Fig. 6; Table 1). The defects could be separated into two groups: lines with a majority of projections missing (either longitudinal or commissural) (Fig. 6B-F), and lines with apparently intact, but mispositioned class IV axons (Fig. 6J-O). The first group included the transcription factor *prospero (pros*; four alleles), l(3)3456 (two alleles), l(3)3425 (three alleles) and l(3)7, l(3)12563 and l(3)12580 (one allele each). Two additional lines, l(3)2332 (Fig. 6E) and a mutant that we named *boojum* (*bum*; Fig. 6F,H) after the similarity between the dendrite phenotype and the shape of the Mexican desert tree, were the only lines with absent commissural branches. Based on complementation studies, neither was allelic to *comm* (data not shown). We examined *bum* further, and found that embryos showed severe dendritic growth defects (Fig. 6G-H). Fas II-labeled fascicles in the CNS were not grossly disrupted in *bum* mutants, although staining was unusually strong in cell bodies throughout the CNS (data not shown). Labeling of *bum* mutants with BP102 showed that an overall normal axon scaffold lost integrity in a posterior-to-anterior progression during embryonic development (Fig. 6I). *bum* therefore appears to affect multiple aspects of neuronal morphology, including midline crossing and mediolateral positioning of axons, and growth and arborization of dendrites. These phenotypes may be due to general defects in the maintenance of dendrite and axon morphology. Based on the anatomical data presented above (Figs 1-3), and preliminary analysis of mutant phenotypes, this first group of sensory axon phenotypes could arise by a failure of axon branching and growth, a failure of commissural and longitudinal branches to segregate, or a failure in axon or dendrite maintenance. Further studies of these mutants, including their autonomous or non-autonomous effects on axon and dendrite morphology, should contribute to our understanding of the molecular control of these events.

The second broad category of mutations included those with more subtly mispositioned axons. We isolated several mutations that affect the integrity and coherence of sensory axon projections (Fig. 6J-O, Table 1). l(3)11534, l(3)1025, l(3)9573 and l(3)10363 (Fig. 6J-M) showed a grossly normal scaffold, but showed extensive defasciculation or disorganization of longitudinal projections. We mapped mutations in l(3)9573 to *brahma* (*brm*), a transcriptional activator related to yeast SNF2/SWI2 (Tamkun et al., 1992) and in l(3)10363 to *protein tyrosine phosphatase 69D* (Desai et al., 1996). The cell autonomy of these mutant phenotypes and other lines has yet to be fully characterized. We also isolated a complementation group consisting of four alleles that we named *baobab* (*boa*) for the frequent inverted class IV axon thickenings (Fig. 6N-O). Dendrites were not disrupted in *boa* mutants (Fig. 6P). Labeling of the *boa* axon scaffold with BP102 revealed weakly labeled longitudinal and commissural tracts, suggesting that this mutation may generally affect axon development (Fig. 6Q).

Given that class IV axons usually terminate in a tract next to class III and II axons, further mosaic studies of mutations in which class IV axons are severely unbundled or laterally displaced might provide insight into the development of axon patterning. We suspect that the high sensitivity of our screen will allow the identification and characterization of genes not previously implicated in neuronal morphogenesis.

DISCUSSION

Representation of somatosensory axons in the CNS: relating dendrite morphology to sensory function

Insect sensory systems, including visual, olfactory, gustatory and somatosensory, represent the external world as sensory maps in the CNS. The nature of the map varies with sensory system (Blagburn and Bacon, 2004). Visual systems retain a map of sensory position in their central axonal projections. The axons of olfactory receptor neurons project to similar positions in the brain if they express the same odorant receptor, and thus transform information about

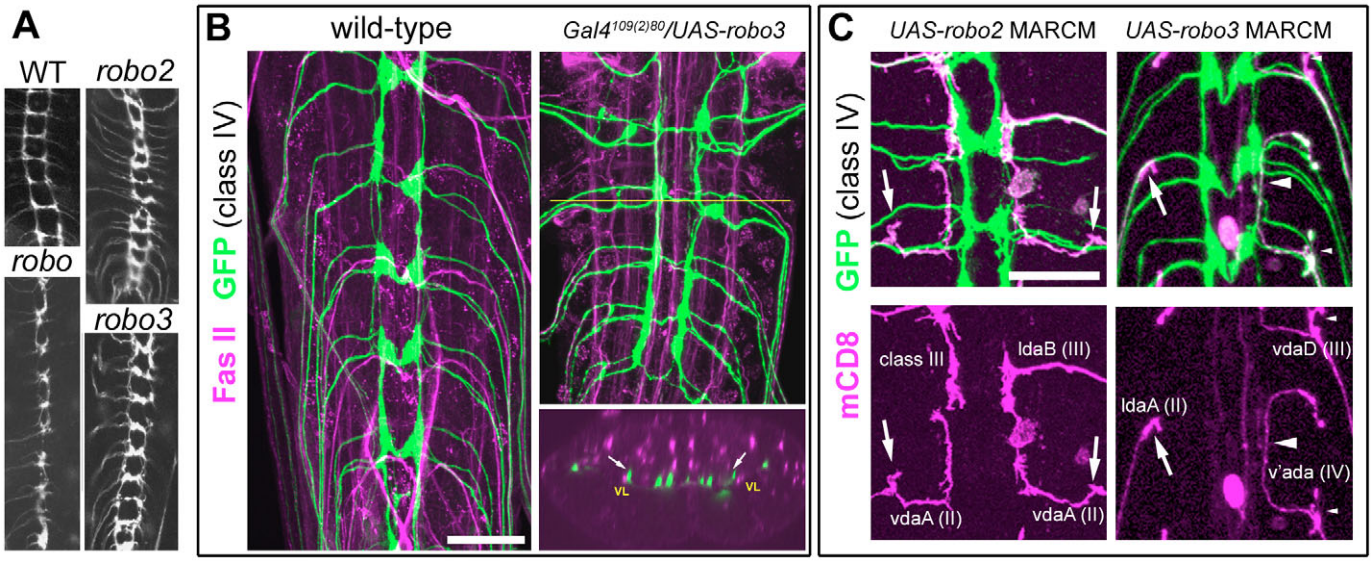

Fig. 5. Study of Robo family members in sensory axon patterning. (**A**) Dorsal view of *ppk-eGFP* pattern in *robo*, *robo2* and *robo3* mutants show abnormal commissure formation or longitudinal branching. (**B**) Wild-type class IV axon scaffold in dorsal view (left) and Robo3 misexpression under the control of the pan-da neuron driver *Gal4*$^{109(2)80}$ (right). Robo3 induces ectopic collateral branch formation at the VL fascicle (arrows) and loss of some midline crossing by class IV neurons. Neurons are visualized using *ppk-eGFP*. (**C**) Robo2 misexpression in single neurons using MARCM does not cause disruptions in axon terminal layering or axon morphology (left panels). Shown are two class III neurons that terminate immediately next to the class IV axon scaffold, and two class II neurons that are separated from the class IV scaffold by a narrow space (arrows point to the collateral branches of the class II neurons). Robo3 misexpression causes defects in axon morphology in class II, III and IV neurons (right panels). The class II neuron ldaA truncates its arbor before reaching its usual position (arrow). Class III and class IV neurons show ectopic collateral branching (small arrowheads). The class IV neuron v′ada reaches a medial position comparable to wild-type class IV axons, but projects laterally in the next anterior segment when forced to express Robo3 (large arrowhead). Genotypes: (B) *yw;Gal4*$^{109(2)80}$*/+* or *Gal4*$^{109(2)80}$*/UAS-robo3; ppk-eGFP/+;* (C) *yw/hsFLP; UAS-robo2* or *robo3/Gal4*$^{109(2)80}$*, UAS-mCD8::GFP; ppk-EGFP th st FRT2A/tubP-Gal80, FRT2A*. Scale bars: 25 μm in B,C.

stimulus quality into a spatial map (Gao et al., 2000b; Vosshall et al., 2000). Gustatory projections retain aspects of both stimulus location and quality in their map (Wang et al., 2004).

Much of our knowledge about somatotopic maps in insect mechanosensory systems derives from studies of bristle afferents with peripheral receptive fields that approximate a point source. *Drosophila* da neurons have largely overlapping peripheral sensory fields and may, as a group, respond to several distinct stimuli (Grueber et al., 2002). How is information from this predominant body wall sensory system represented in the CNS and what might this organization tell us about the possible functions of da neurons? We show that neurons with different dendritic branching morphologies target distinct regions of the CNS, supporting the existence of a modality map of da neuron axons. We further provide evidence for nested somatotopic mapping in class I and class IV da neurons. Individual class I neurons extend their dendritic and axonal arbors in the same preferred direction along the AP body axis (Fig. 1C). Class IV axons project across the midline according to the cell body position along the DV axis of the body wall, with dorsal and ventral cells, but not more lateral cells, crossing the midline. It is possible that class II and III neurons also project in a somatotopic pattern that was not uncovered by our analysis. Thus, da neuron connectivity appears to incorporate both class and position-specific components, with some apparent correlations with dendritic field orientation.

In the context of sensory processing, these data suggest distinct functions for different morphological classes of da neurons. The class II-IV neurons target a ventral region of the neuropil; thus information from these neurons might be processed similarly to ventral-projecting tactile sensory bristle neurons (Schrader and Merritt, 2000). Within this ventral region, the class-specific laminar pattern could allow differential connectivity with second-order interneurons. Additionally, class II neurons, with their collateral branches, might provide information to distinct central circuits. The class I neurons targeted a more dorsal region of the neuropil, which is generally a characteristic of proprioceptive afferents in insects (Merritt and Murphey, 1992; Murphey et al., 1989; Pfluger et al., 1988; Schrader and Merritt, 2000). Indeed, a class of da neurons in *Manduca* has been shown to target dorsal neuropil, and to respond to stretch of the cuticle (Grueber et al., 2001). Many insect proprioceptors, including chordotonal organs and the bipolar dendrite neurons, have dendrites oriented in a preferential direction relative to the body axis. Notably, the primary dendrites of each class I neuron are oriented dorsally and secondary dendrites are oriented anteriorly and posteriorly (Grueber et al., 2002). This arrangement could allow larvae to compare distension along major body axes. While the anatomical arrangement of their axons suggests distinct functions for different da neurons, dissecting these different functions will ultimately require behavioral and physiological studies (Ainsley et al., 2003; Liu et al., 2003; Tracey et al., 2003).

Mechanisms of class-specific axon and dendrite patterning

A notable feature of the mapping of da sensory afferents is their predominant organization into class-correlated mediolateral layers (Figs 2, 3), with class IV neurons in a medial layer, class III neurons intermediate, and class II neurons most lateral. These layers do not correspond to the medial, intermediate and lateral fascicles that have their position specified by a Robo combinatorial code (Rajagopalan et al., 2000; Simpson et al., 2000); thus novel molecular cues may

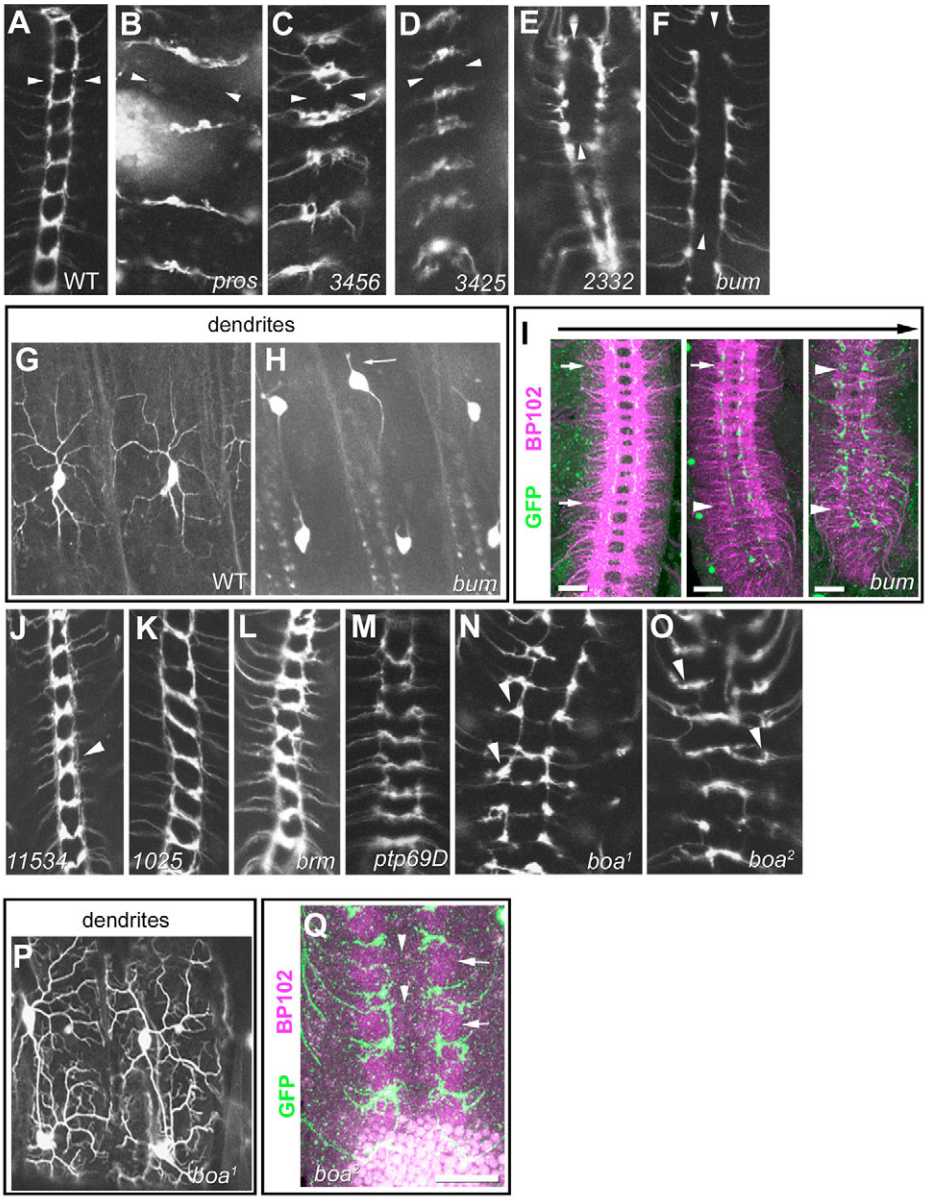

Fig. 6. A mutagenesis screen identifies sensory axon and dendrite arborization phenotypes. (**A**) Wild-type class IV embryonic axon scaffold visualized by *ppk-eGFP*. (**B-D**) Defects in longitudinal branch formation shown by lines isolated from the screen. Arrowheads in B-D indicate missing longitudinal tracts. (**E**) l(3)2332 mutants show loss of most commissural branches. (**F**) *boojum* (*bum*) mutants show loss of commissural axon branching in the CNS and highly reduced dendritic branching (**G**,**H**). Arrowheads in E-F indicate missing commissural branches. Arrows in H indicate stunted dendritic arbors. (**I**) Labeling with the axonal marker BP102 shows that despite the lack of sensory axon commissural branches, commissural tracts seem to develop normally but undergo a successive loss of labeling or integrity during development. Temporal progresssion is inferred by gut morphology and VNC length. Arrows indicate grossly intact areas of the VNC; arrowheads indicate areas that are disrupted. (**J-O**) Mutations disrupting axon tract coherence or position. Lines l(3)11534 (J) and l(3)1025 (K) lack a coherent longitudinal axon tract (arrowhead). (L-M) Mutations in *brahma* (*brm*), a chromatin remodeling factor, show defasciculation or thinning of longitudinal tracts. (N-O) Axon phenotype of two *boa* alleles. Note that axons generally branch lateral to, rather than between, longitudinal branches (arrowheads). (**P**) *boa* mutants show no obvious abnormalities in dendrite morphology. (**Q**) Staining of *boa*^{2} mutants with the axonal marker BP102 reveals the presence of longitudinal (arrows) and commissural (arrowhead) tracts but relatively weak labeling. Anterior is up in CNS images. Dorsal is up in PNS images. Animals are stage 17 except E,P, which are hatchling larvae. Scale bars: 25 μm in I,Q.

contribute to this laminar organization. Indeed, it has been postulated that the Robo code provides information about the broad zone that a growth cone targets, while a complementary fasciculation code fine-tunes pathway choice within that zone (Rajagopalan et al., 2000). It is conceivable that Robo proteins could participate in specifying the lateral position of collateral branches, as Robo3 overexpression in individual neurons induced ectopic branching from the axon shaft. Although we did not detect cell-type-specific expression of Robo3 in neurons that normally show such branching, it is notable that Robo3 has been implicated in cell-type-specific patterning decisions of PNS axons (Zlatic et al., 2003), and that Slit2 has been proposed as a positive regulator of collateral branching of dorsal root ganglion sensory axons (Wang et al., 1999).

The mechanisms for targeting of somatosensory afferents should act to properly position axons of different classes relative to one another. Several alternative mechanisms could contribute to this positioning. One potentially important component of axon sorting could involve interactions between homotypic or heterotypic axons. Heterotypic axons could repel each other to sort to discrete bundles. Likewise, homotypic axons could adhere to one another to ensure that they terminate together. Olfactory receptor neuron axons engage in extensive hierarchical interactions to establish precise targeting in olfactory glomeruli (Komiyama et al., 2004), and dendrites of da neurons engage in class-selective interactions during development to ensure their proper spacing (Grueber et al., 2003b; Sugimura et al., 2003). It is therefore conceivable that intraclass and interclass interactions could participate in the sorting of somatosensory axons. Axons from different classes could also project to specific layers that are prepatterned by the processes of target interneurons or by other axons. Finally, the projection of da axons to different layers could conceivably reflect a temporal order of sensory axon arrival in the CNS, similar to the three-way correlation between mediolateral axon position, physiological function and time of differentiation among *Drosophila* wing campaniform sensilla (Palka et al., 1986). Among the ventral cluster da neurons, a group with differentiation that has been examined in the greatest detail, the class II neurons appear to be the first-born, followed by class III neurons and class IV neurons (Orgogozo et al., 2001). These data suggest a possible correlation

Table 1. Dendrite and axon phenotypes of EMS-induced third-chromosome mutation, as assessed in *ppk-eGFP* embryos

Gene/mutation	Phenotype		Cytology	Alleles
	Dendrite	Axon		
l(3)1025	None	Defasciculation	61A;66D10	1
ptp69D	B	Defasciculation	69D6;69E1	1
l(3)9374	B	Defasciculation	86D3; 90E4	1
dally	G	Disorganization	66E1-3	1
brahma	B	Disorganization	72C1	1
l(3)8172 (*fng*)**	G	Disrupted longitudinals*	78A1	1
Scm	None	Disrupted longitudinals*	85E2	1
l(3)3425	R, B	Missing longitudinals	72D1;86D3	3
pros	R	Missing longitudinals	86E2-4	4
l(3)3456	None	Missing longitudinals	93C7;100F5	2
rhomboid	None	Fused longitudinals	62A2	2
sim	None	Fused longitudinals	87D11	2
boojum	G	No commissures	77A1;77D1	1
l(3)2332	None	Missing commissures	Not determined	1
boa	None	Missing/ectopic axon branches	95F7;96A18	4
trc	T, B	None	76D1	2
l(3)2727	R	None	89E1;91B2	2

B, branching; G, growth; R, routing; T, tiling.
*Occasional loss of longitudinal and commissural branches.
**Mutation detected in *fringe* but, by complementation analysis, may not account for the complete phenotype.

between birth order and axon position in the neuropil, although additional early markers of da neurons and further high-resolution imaging studies are required to further test this scenario.

The molecular basis for insect sensory neuron differentiation, as well as anatomical studies of somatosensory axon mapping and VNC circuitry, have been subjects of considerable study (Blagburn and Bacon, 2004), and principles are emerging that link the two areas into molecular models of connectivity and synaptic specificity (Merritt et al., 1993; Merritt and Whitington, 1995; Nottebohm et al., 1992; Zlatic et al., 2003). Among embryonic sensory neurons in *Drosophila*, there is a three-way correlation between soma position, proneural transcription factor expression and axon projection pattern, suggesting that these transcription factors may endow aspects of modality-specific axonal projections (Merritt and Whitington, 1995). Such a link was recently established between chordotonal-organ-specific expression of the *atonal* proneural gene and expression of the Robo3 axon guidance molecule in these same organs (Zlatic et al., 2003). Misexpression experiments with *atonal*, *robo3* and *comm* suggest a model whereby Atonal activates expression of Robo3, which in turn specifies mediolateral positioning in chordotonal versus bipolar dendrite-type axon projections (Zlatic et al., 2003). These studies provide an important basis for understanding the establishment of sensory circuitry in the VNC.

To begin to address the molecular basis of axon and dendrite patterning using the anatomical framework established for the da neurons, we undertook a forward genetic approach, which has proven a successful means to identify regulators of neuronal morphogenesis (Gao et al., 1999; Lee et al., 2000; Reuter et al., 2003). A strength of this screen was the ability to simultaneously assess phenotypes in dendrites and axons at the level of single identifiable neurons. We have identified numerous complementation groups that affect axon patterning, including several mutations with a molecular nature as yet unknown (see Table 1). These mutations should allow us to identify new genes involved in axon morphogenesis and place these into the context of their effects on somatosensory axon patterning and circuitry. Given that we further identified many mutations affecting dendrite morphogenesis (Table 1), we expect that studies of the mutations identified from the screen will also allow us to address the similarities and distinctions between axon and dendrite development.

We thank Atsushi Miyawaki for Kaede plasmid; Barry Dickson, Kei Ito, Graeme Mardon, Veronica Rodrigues, Kristin Scott, Jessica Treisman, David Van Vactor, Marta Zlatic and the Bloomington Stock Center for fly stocks; Zuoren Wang for helpful advice on using the FLP-out system; Fabrice Roegiers for assistance in making the UAS-Kaede lines; and members of the Jan lab for comments. W.B.G. thanks members of his laboratory for comments and assistance during later stages. Supported by NIH R01 NS 40929 (Y-N.J.) and Kirschstein NRSA fellowships F32-NS43027 (W.B.G.), F32 NS46847 (B.Y.) and the Jane Coffin Childs Foundation (C-H.Y.). Y-N.J. and L.Y.J. are Investigators of the Howard Hughes Medical Institute.

References

Ainsley, J. A., Pettus, J. M., Bosenko, D., Gerstein, C. E., Zinkevich, N., Anderson, M. G., Adams, C. M., Welsh, M. J. and Johnson, W. A. (2003). Enhanced locomotion caused by loss of the Drosophila DEG/ENaC protein Pickpocket1. *Curr. Biol.* **13**, 1557-1563.

Ando, R., Hama, H., Yamamoto-Hino, M., Mizuno, H. and Miyawaki, A. (2002). An optical marker based on the UV-induced green-to-red photoconversion of a fluorescent protein. *Proc. Natl. Acad. Sci. USA* **99**, 12651-12656.

Basler, K. and Struhl, G. (1994). Compartment boundaries and the control of Drosophila limb pattern by hedgehog protein. *Nature* **368**, 208-214.

Blagburn, J. M. and Bacon, J. P. (2004). Control of central synaptic specificity in insect sensory neurons. *Annu. Rev. Neurosci.* **27**, 29-51.

Bodmer, R. and Jan, Y. N. (1987). Morphological differentiation of the embryonic peripheral neurons in drosophila. *Roux's Arch. Dev. Biol.* **196**, 69-77.

Brenman, J. E., Gao, F. B., Jan, L. Y. and Jan, Y. N. (2001). Sequoia, a tramtrack-related zinc finger protein, functions as a pan-neural regulator for dendrite and axon morphogenesis in Drosophila. *Dev. Cell* **1**, 667-677.

Gao, F. B., Brenman, J. E., Jan, L. Y. and Jan, Y. N. (1999). Genes regulating dendritic outgrowth, branching, and routing in Drosophila. *Genes Dev.* **13**, 2549-2561.

Gao, F. B., Kohwi, M., Brenman, J. E., Jan, L. Y. and Jan, Y. N. (2000a). Control of dendritic field formation in Drosophila: the roles of flamingo and competition between homologous neurons. *Neuron* **28**, 91-101.

Gao, Q., Yuan, B. and Chess, A. (2000b). Convergent projections of Drosophila olfactory neurons to specific glomeruli in the antennal lobe. *Nat. Neurosci.* **3**, 780-785.

Grueber, W. B., Graubard, K. and Truman, J. W. (2001). Tiling of the body wall by multidendritic sensory neurons in Manduca sexta. *J. Comp. Neurol.* **440**, 271-283.

Grueber, W. B., Jan, L. Y. and Jan, Y. N. (2002). Tiling of the Drosophila epidermis by multidendritic sensory neurons. *Development* **129**, 2867-2878.

Grueber, W. B., Jan, L. Y. and Jan, Y. N. (2003a). Different levels of the homeodomain protein cut regulate distinct dendrite branching patterns of Drosophila multidendritic neurons. *Cell* **112**, 805-818.

Grueber, W. B., Ye, B., Moore, A. W., Jan, L. Y. and Jan, Y. N. (2003b). Dendrites of distinct classes of Drosophila sensory neurons show different capacities for homotypic repulsion. *Curr. Biol.* **13**, 618-626.

Komiyama, T., Carlson, J. R. and Luo, L. (2004). Olfactory receptor neuron axon

targeting: intrinsic transcriptional control and hierarchical interactions. *Nat. Neurosci.* **7**, 819-825.
Komiyama, T., Johnson, W.A., Luo, L. and Jefferis, G.S. (2003). From lineage to wiring specificity. POU domain transcription factors control precise connections of *Drosophila* olfactory projection neurons. *Cell* **112**, 157-167.
Landgraf, M., Sanchez-Soriano, N., Technau, G. M., Urban, J. and Prokop, A. (2003). Charting the Drosophila neuropile: a strategy for the standardised characterisation of genetically amenable neurites. *Dev. Biol.* **260**, 207-225.
Lee, T. and Luo, L. (1999). Mosaic analysis with a repressible cell marker for studies of gene function in neuronal morphogenesis. *Neuron* **22**, 451-461.
Lee, T., Marticke, S., Sung, C., Robinow, S. and Luo, L. (2000). Cell-autonomous requirement of the USP/EcR-B ecdysone receptor for mushroom body neuronal remodeling in Drosophila. *Neuron* **28**, 807-818.
Levine, R. B., Pak, C. and Linn, D. (1985). The structure, function, and metamorphic reorganization of somatotopically projecting sensory neurons in Manduca sexta larvae. *J. Comp. Physiol. A* **157**, 1-13.
Lewis, E.B. and Bacher, F. (1968). Methods of feeding ethyl methane sulphonate (EMS) to *Drosophila* males. *Dros. Inf. Serv.* **43**, 193-194.
Li, W., Wang, F., Menut, L. and Gao, F. B. (2004). BTB/POZ-zinc finger protein abrupt suppresses dendritic branching in a neuronal subtype-specific and dosage-dependent manner. *Neuron* **43**, 823-834.
Liu, L., Yermolaieva, O., Johnson, W. A., Abboud, F. M. and Welsh, M. J. (2003). Identification and function of thermosensory neurons in Drosophila larvae. *Nat. Neurosci.* **6**, 267-273.
Marin, E. C., Jefferis, G. S., Komiyama, T., Zhu, H. and Luo, L. (2002). Representation of the glomerular olfactory map in the Drosophila brain. *Cell* **109**, 243-255.
Merritt, D. J. and Murphey, R. K. (1992). Projections of leg proprioceptors within the CNS of the fly Phormia in relation to the generalized insect ganglion. *J. Comp. Neurol.* **322**, 16-34.
Merritt, D. J. and Whitington, P. M. (1995). Central projections of sensory neurons in the Drosophila embryo correlate with sensory modality, soma position, and proneural gene function. *J. Neurosci.* **15**, 1755-1767.
Merritt, D. J., Hawken, A. and Whitington, P. M. (1993). The role of the cut gene in the specification of central projections by sensory axons in Drosophila. *Neuron* **10**, 741-752.
Moore, A. W., Jan, L. Y. and Jan, Y. N. (2002). hamlet, a binary genetic switch between single- and multiple-dendrite neuron morphology. *Science* **297**, 1355-1358.
Murphey, R. K., Possidente, D., Pollack, G. and Merritt, D. J. (1989). Modality-specific axonal projections in the CNS of the flies Phormia and Drosophila. *J. Comp. Neurol.* **290**, 185-200.
Nottebohm, E., Dambly-Chaudiere, C. and Ghysen, A. (1992). Connectivity of chemosensory neurons is controlled by the gene poxn in Drosophila. *Nature* **359**, 829-832.
Orgogozo, V., Schweisguth, F. and Bellaiche, Y. (2001). Lineage, cell polarity and inscuteable function in the peripheral nervous system of the Drosophila embryo. *Development* **128**, 631-643.
Palka, J., Malone, M. A., Ellison, R. L. and Wigston, D. J. (1986). Central projections of identified Drosophila sensory neurons in relation to their time of development. *J. Neurosci.* **6**, 1822-1830.
Pfluger, H. J., Braunig, P. and Hustert, R. (1988). The organization of mechanosensory neuropiles in locust thoracic ganglia. *Philos. Trans. R. Soc. London Ser. B* **321**, 1-26.
Rajagopalan, S., Vivancos, V., Nicolas, E. and Dickson, B. J. (2000). Selecting a longitudinal pathway: Robo receptors specify the lateral position of axons in the Drosophila CNS. *Cell* **103**, 1033-1045.
Reuter, J. E., Nardine, T. M., Penton, A., Billuart, P., Scott, E. K., Usui, T., Uemura, T. and Luo, L. (2003). A mosaic genetic screen for genes necessary for Drosophila mushroom body neuronal morphogenesis. *Development* **130**, 1203-1213.
Schrader, S. and Merritt, D. J. (2000). Central projections of Drosophila sensory neurons in the transition from embryo to larva. *J. Comp. Neurol.* **425**, 34-44.
Sharma, Y., Cheung, U., Larsen, E. W. and Eberl, D. F. (2002). PPTGAL, a convenient Gal4 P-element vector for testing expression of enhancer fragments in drosophila. *Genesis* **34**, 115-118.
Simpson, J. H., Bland, K. S., Fetter, R. D. and Goodman, C. S. (2000). Short-range and long-range guidance by Slit and its Robo receptors: a combinatorial code of Robo receptors controls lateral position. *Cell* **103**, 1019-1032.
Sugimura, K., Satoh, D., Estes, P., Crews, S. and Uemura, T. (2004). Development of morphological diversity of dendrites in Drosophila by the BTB-zinc finger protein abrupt. *Neuron* **43**, 809-822.
Sugimura, K., Yamamoto, M., Niwa, R., Satoh, D., Goto, S., Taniguchi, M., Hayashi, S. and Uemura, T. (2003). Distinct developmental modes and lesion-induced reactions of dendrites of two classes of *Drosophila* sensory neurons. *J. Neurosci.* **23**, 3752-3760.
Sweeney, N. T., Li, W. and Gao, F. B. (2002). Genetic manipulation of single neurons in vivo reveals specific roles of flamingo in neuronal morphogenesis. *Dev. Biol.* **247**, 76-88.
Tamkun, J. W., Deuring, R., Scott, M. P., Kissinger, M., Pattatucci, A. M., Kaufman, T. C. and Kennison, J. A. (1992). brahma: a regulator of Drosophila homeotic genes structurally related to the yeast transcriptional activator SNF2/SWI2. *Cell* **68**, 561-572.
Tracey, W. D., Jr, Wilson, R. I., Laurent, G. and Benzer, S. (2003). painless, a Drosophila gene essential for nociception. *Cell* **113**, 261-273.
Vosshall, L. B., Wong, A. M. and Axel, R. (2000). An olfactory sensory map in the fly brain. *Cell* **102**, 147-159.
Wang, K. H., Brose, K., Arnott, D., Kidd, T., Goodman, C. S., Henzel, W. and Tessier-Lavigne, M. (1999). Biochemical purification of a mammalian slit protein as a positive regulator of sensory axon elongation and branching. *Cell* **96**, 771-784.
Wang, Z., Singhvi, A., Kong, P. and Scott, K. (2004). Taste representations in the Drosophila brain. *Cell* **117**, 981-991.
Wong, A. M., Wang, J. W. and Axel, R. (2002). Spatial representation of the glomerular map in the Drosophila protocerebrum. *Cell* **109**, 229-241.
Ye, B., Petritsch, C., Clark, I. E., Gavis, E. R., Jan, L. Y. and Jan, Y. N. (2004). Nanos and Pumilio are essential for dendrite morphogenesis in Drosophila peripheral neurons. *Curr. Biol.* **14**, 314-321.
Zlatic, M., Landgraf, M. and Bate, M. (2003). Genetic specification of axonal arbors: atonal regulates robo3 to position terminal branches in the Drosophila nervous system. *Neuron* **37**, 41-51.